Hindawi
Geofluids
Volume 2023, Article ID 4761786, 19 pages
https://doi.org/10.1155/2023/4761786

Research Article

Investigation of Rock Mechanical Properties under Liquid Nitrogen Environment

Linchao Wang,[1] Xin Liang,[1] Xuyang Shi,[2] Jianyong Han,[3] Yang Chen,[1] and Wan Zhang[1]

[1]*School of Civil Engineering and Architecture, Xi'an University of Technology, Xi'an 710048, China*
[2]*School of Mechanics and Civil Engineering, China University of Mining and Technology, Xuzhou 221116, China*
[3]*School of Civil Engineering, Shandong Jianzhu University, Jinan 250101, China*

Correspondence should be addressed to Xin Liang; xliang@xaut.edu.cn and Xuyang Shi; sxywlp2008@163.com

Received 25 August 2023; Revised 3 December 2023; Accepted 14 December 2023; Published 29 December 2023

Academic Editor: Zetian Zhang

In order to promote sustainable energy development and reduce the impact of fossil fuels on the environment, it is crucial to strengthen the development and utilization of clean and renewable geothermal energy. Liquid nitrogen fracturing, as an emerging waterless fracturing technology, has outstanding advantages in rock fracturing effect and thermal exchange ability with hot dry rock and is more environmentally friendly. In order to evaluate the influence of liquid nitrogen on the mechanical properties, acoustic emission characteristics, and cross-sectional crack propagation characteristics of granite at different initial temperatures, this paper carried out three-point bending tests and acoustic emission detection on granite treated by high-temperature heating and liquid nitrogen cooling. Finally, based on the cross-sectional scanning test, the expansion characteristics of microcracks in granite were analyzed. The results show that the higher the initial temperature of granite, the stronger the cold impact of liquid nitrogen on granite, and the faster the rock's mechanical performance declines. The acoustic emission ringing count is closely related to the development of microcracks in granite, and as the initial temperature of granite increases, the more ringing counts there are, indicating that the huge temperature difference induces more microcracks inside the rock. In addition, the cold impact of liquid nitrogen can effectively promote the fracturing of granite. After liquid nitrogen treatment, the fractal dimension of the granite cross-section increases, the shape of the cross-section becomes rough, and many micropores appear. This study can provide a scientific basis for the engineering application of liquid nitrogen fracturing technology.

1. Introduction

Energy serves as the cornerstone and impetus for human survival and progress, carrying profound implications for national security and societal welfare. Its pivotal role in fostering economic and social advancement and enhancing the quality of life for individuals cannot be overemphasized. Since the first Industrial Revolution that began in the 1860s, energy has emerged as a critically important strategic resource in history [1, 2]. With sustained rapid economic growth, there has been a relentless increase in global energy demand. The increasing utilization of nonrenewable resources like oil and coal has resulted in challenges related to resource scarcity and global climate change. Consequently, there is an urgent need to prioritize the development and utilization of clean and renewable energy sources as a measure that effectively balances economic progress with environmental conservation [3–5].

With the growing global demand for clean and renewable energy, there is an urgent need to find alternative ways to fossil fuels and reduce their negative impact on the environment. In this regard, geothermal energy is widely regarded as a highly promising renewable energy source. China has abundant and widely distributed geothermal energy resources, which have excellent application prospects. Through in-depth research on the development of

geothermal resources, we can promote energy transformation, reduce dependence on traditional energy sources, reduce environmental pollution, protect the ecological environment of the Earth, and provide more reliable energy supply for sustainable development. One of the crucial challenges in geothermal energy development and utilization is the efficient fracturing and creation of flow channels within hot dry rock reservoirs. Hydraulic fracturing, thermal stimulation, and chemical stimulation are commonly used methods for inducing fractures in current practice [6–10]. Among these, hydraulic fracturing is the most effective and commonly employed technique in practical engineering, especially in oil and gas operations. However, in actual engineering applications, hydraulic fracturing often results in the formation of a single large fracture in the hot dry rock, leading to a smaller heat exchange area, contrary to the original intention of enhanced geothermal system (EGS) projects. Furthermore, conventional hydraulic fracturing methods come with a set of limitations, such as the uncertain positioning of rock fractures, the risk of environmental contamination, and the possibility of induced seismic activities [11, 12].

As an innovative waterless fracturing technique, liquid nitrogen fracturing has shown broad application prospects in the development of hot dry rock reservoirs [13]. Using liquid nitrogen as a fracturing fluid has several advantages. When applied to hot dry rocks, liquid nitrogen induces crack formation by applying pressure and generates intense thermal stress due to the significant temperature difference between the nitrogen and the rocks [14]. Therefore, the formation of numerous thermally induced cracks greatly enhances the fracturing process within the reservoir. Additionally, liquid nitrogen fracturing has advantages such as using local resources, being nonpolluting, and better heat exchange with hot dry rocks. Compared to traditional fracturing methods, it is more efficient and environmentally friendly, making it an important technology for promoting the exploitation of geothermal resources.

Grundmann et al., Coetzee et al., McDaniel et al., Rassenfoss, and Cha et al. have conducted relevant research on liquid nitrogen fracturing from various perspectives [15–19]. In their experimental study, Grundmann et al. [15] observed a notable 8% enhancement in gas production rates achieved through the implementation of liquid nitrogen fracturing in shale formations. Similarly, Coetzee et al. [16] found that using liquid nitrogen as a fracturing fluid effectively improves rock fracturing, resulting in accelerated generation and development of fractures. In their research, McDaniel et al. [17] investigated the thermal impact resulting from injecting liquid nitrogen into coal-bed methane reservoirs and found that this effect effectively prevents the closure of thermally induced and hydraulic fractures, highlighting an orthogonal relationship between the two. Rassenfoss [18] validated the influence of thermal impact on rocks during liquid nitrogen fracturing and elaborated on it in their publication. Cha et al. [19] elucidated the underlying mechanism of internal rock damage caused by liquid nitrogen, attributing it to temperature gradients and the cold impact resulting from the interaction between liquid nitrogen and rocks. In their study, Cai et al. [20] performed a series of mechanical experiments to investigate the impact of liquid nitrogen cooling on the mechanical properties and surface modifications of rocks. The researchers examined the mechanisms behind rock fracturing induced by liquid nitrogen and its influence on the rock failure process. Moreover, they explored the benefits and potential applications of liquid nitrogen fracturing technology in the field of oil and gas engineering. The researchers proposed and verified an enhanced production technique called jet fracturing with liquid nitrogen, which demonstrated significant advantages over conventional liquid nitrogen fracturing methods. In addition, they conducted liquid nitrogen fracturing experiments using a self-designed testing apparatus, studying the fracturing mechanism of shale under liquid nitrogen and proposing a novel operational approach known as the alternate operation of liquid nitrogen freezing and nitrogen fracturing.

Lai et al. [21] examined the suitability of liquid nitrogen for the advancement of hot dry rock geothermal resources and arrived at favorable findings. They summarized the mechanisms and key technologies of rock fracturing using liquid nitrogen, highlighting its advantages in efficient rock breaking and effective extraction of reservoir thermal energy. Li et al. [22] introduced a novel fracturing technique called liquid nitrogen gasification fracturing, which is applicable for low-permeability oil and gas reservoirs. In their study, Zhang et al. [23] utilized laser microscopy to observe the impact of liquid nitrogen cooling on coal samples. Their findings revealed that the application of liquid nitrogen cooling causes thermal stress and stress concentration, leading to the formation and propagation of microfractures within the original specimens. As a result, coal permeability is greatly enhanced. Zhang et al. [24] conducted semi-immersion experiments with liquid nitrogen to analyze its enhanced fracturing and permeability improvement effects on coal. The results indicated that liquid nitrogen fracturing can effectively enhance coal permeability. Wang et al. [25] conducted experiments on liquid nitrogen fracturing of coal and found that heating the coal and cooling it with liquid nitrogen effectively reduce the initiation pressure for coal fracturing. Scanning electron microscopy (SEM) results indicated that the low-temperature characteristics of liquid nitrogen make the coal more prone to intergranular and transgranular fractures, thereby improving the effectiveness of coal fracturing. Li et al. [26] studied the impact of liquid nitrogen freezing treatment on the pore structure of coal and found that it can effectively enhance the coal's pore structure. After freezing, the total pore volume of the coal increased significantly, pore connectivity was enhanced, and the pore distribution became more uniform. Therefore, liquid nitrogen fracturing technology can effectively improve the permeability of coal seams. Khurshid et al. [27] analyzed the impact of organic particle deposition on reservoir fractures and the permeability of reservoir rock matrix by establishing a numerical model.

Currently, many scholars are actively researching the feasibility and practical effects of the liquid nitrogen fracturing technology, and a series of research achievements have been made. However, geothermal resources are mainly

distributed in specific regions such as volcanic areas and earthquake zones. Geothermal exploitation faces multiple technical challenges such as high temperatures, high pressure, and corrosion, which makes the commercial application of geothermal resources yet to be achieved. In addition, most of the research on liquid nitrogen fracturing technology is still at the stage of indoor experiments and numerical simulation. There is no clear conclusion about the specific application effects of liquid nitrogen fracturing technology in actual engineering. Therefore, to truly apply the liquid nitrogen fracturing technology in actual engineering, a large amount of sufficient experimental research is still needed.

In summary, scholars have conducted extensive research on liquid nitrogen-induced fracturing of rocks. Building upon previous studies, this paper investigates the cold impact effect of liquid nitrogen on high-temperature granite through high-temperature heating and liquid nitrogen cooling treatments. Subsequently, the treated granite is subjected to three-point bending tests, acoustic emission detection, and cross-sectional scanning experiments to evaluate the mechanical properties, acoustic emission characteristics, and cross-sectional crack propagation influenced by liquid nitrogen at different initial temperatures. We also explore the fracture toughness and microcrack propagation characteristics of granite under different temperature gradients. These research findings provide new evaluation methods and references for the engineering development of geothermal resources.

2. Instrumentation and Experimental Design

2.1. Preparation of Test Rock Samples. The rock samples utilized in this experiment were sourced from granite located in Xuzhou City, Jiangsu Province, China. In theory, as the Earth gets closer to its core, the temperature increases. Therefore, in any region, geothermal resources can be developed as long as a certain depth can be reached. However, due to cost and technological limitations, currently, humans can only utilize shallow geothermal reservoirs. In other words, with the current technological means, areas of new volcanic activity or regions where the crust has already thinned are the most promising for geothermal resource development. To ensure the validity of the research, it is crucial to carefully choose rocks that exhibit comparable properties, considering the physical characteristics and distribution of low porosity and permeability within geothermal reservoirs. Granite, which is an igneous rock, shares similar physical properties with hot dry rocks, such as its hard texture and low porosity and permeability. Moreover, granite is widely distributed in the Earth's crust and easily accessible. In light of the regional distribution patterns exhibited by hot dry rock-type geothermal resources in China, a granite sample obtained from Xuzhou City, located in Jiangsu Province, was selected for the experiment [28].

Under sealed conditions, the original rock samples were transported to the laboratory for further processing. The resulting processed rock samples can be observed in Figure 1. Furthermore, to mitigate the potential impact of rock heterogeneity on experimental outcomes, all samples

Figure 1: Granite specimen.

were extracted from a single rock mass. The rocks were processed into multiple different core samples for experimentation. For the three-point bending test, a disk-shaped specimen with specific dimensions was employed. Figure 1 presents this specimen, which had a thickness of 30 mm, a diameter of 76 mm, and an artificial notch length of 14 mm. The artificial notch was oriented perpendicular to the bottom edge diameter of the semicircular disk. The surface flatness, preexisting crack width, and perpendicularity of the preexisting crack of the aforementioned samples were within the tolerance range guidelines set forth by the International Society for Rock Mechanics (ISRM) [29].

2.2. Experimental Equipment. This experiment used a domestically produced CSS-44100 testing machine for a three-point bending test. This system can perform various physical and mechanical tests such as the three-point bending test and Brazilian splitting test and can calculate various mechanical parameters of rocks. The system consists of an axial loading system and a computer control system, as shown in Figure 2(a).

The three-dimensional cross-section scanning device employed was the VR-5000 series 3D profilometer. This equipment boasts high precision and is capable of completing measurements in a short period of time, saving over 75% of the time compared to traditional devices. Furthermore, it has the ability to perform surface measurements on rock samples, automatically identifying the height, the width, and the highest and lowest points of the rock mass, as depicted in Figure 2(b).

Acoustic emission measurements were performed using the dedicated PCI-2 acoustic emission system, manufactured by Physical Acoustics Corporation (PAC) based in the United States. This system features an 18-bit A/D converter with a frequency range of 1 kHz to 3 MHz, providing low noise characteristics. The standard PCI card is equipped with a processor and includes 4 high-pass and 6 low-pass filters that can be selectively controlled through software. The system allows for real-time analysis of acoustic emission signals and offers high precision, as depicted in Figure 2(c).

2.3. Experimental Procedure. The granite specimens were divided into two groups and labeled as untreated-1, untreated-2, 25-1, 25-2, 100-1, 100-2, 200-1, 200-2, 300-1,

(a) CSS-44100 testing machine

(b) VR-5000 series 3D profilometer

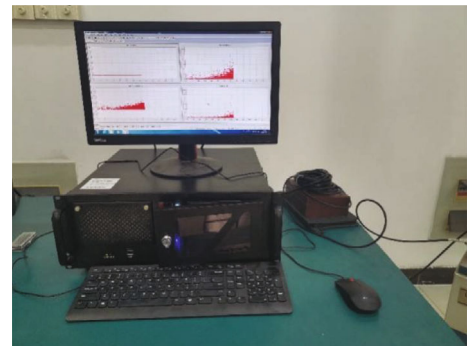

(c) Acoustic emission system PCI-2

Figure 2: Experimental setup.

300-2, 400-1, and 400-2. Each group of specimens underwent different treatments, including untreated at room temperature (25°C), cooling with liquid nitrogen after heating to 100°C, cooling with liquid nitrogen after heating to 200°C, cooling with liquid nitrogen after heating to 300°C, and cooling with liquid nitrogen after heating to 400°C.

The high-temperature heating involved subjecting the specimens to a continuous heat treatment at the predetermined temperature for 3 hours. For liquid nitrogen cooling, the specimens were immersed in liquid nitrogen for a duration of 1 hour. The heating chamber utilized for heating the granite specimens can be seen in Figure 3(a), while Figure 3(b) portrays the liquid nitrogen tank. Furthermore, in order to investigate the impact of high-temperature heating and liquid nitrogen cooling on the internal structure of granite, we employed a nonmetallic ultrasonic monitoring analyzer to conduct ultrasonic testing before and after the experiments. During this process, the emission voltage was set at 500 V, and the sampling period was 0.4 microseconds. By observing the changes in wave velocity, we can directly reflect the degree of damage to the internal structure of the granite.

After the pretreatment of the granite is completed, the specimen is allowed to return to room temperature, followed by a three-point bending test. This test is conducted using displacement control at a loading rate of 0.1 mm/min. Simultaneously with the mechanical testing, acoustic emission detection is carried out to monitor the evolution characteristics of microcracks within the granite in real time. Upon completion of the loading test, fractured granite specimens are subjected to cross-sectional scanning to investigate the roughness and fractal dimension characteristics of the granite fracture surface.

In this experiment, we simulated the conditions of granite under different high-temperature states and in a liquid nitrogen cooling environment. However, it must be acknowledged that the impact of in situ stress in actual engineering scenarios was not considered in this experiment. Additionally, our study only involved one type of rock, namely, granite, and did not encompass other rock types. Therefore, in practical applications, it is necessary to comprehensively consider different types of rocks as well as factors such as in situ stress. This will help to more accurately assess and predict the performance of rocks in actual engineering scenarios.

3. Investigation of Mechanical Behavior of Granite

3.1. Experimental Results of Mechanical Properties of Granite. To examine the mechanical behavior of granite, three-point bending tests were conducted to acquire load-displacement curves at different initial heating temperatures. These curves provide valuable insights into the granite's response under different conditions. Figure 4 presents the load-displacement curves of the granite specimens under varied treatments,

(a) Heating chamber (b) Liquid nitrogen tank

Figure 3: Heating and cooling equipment.

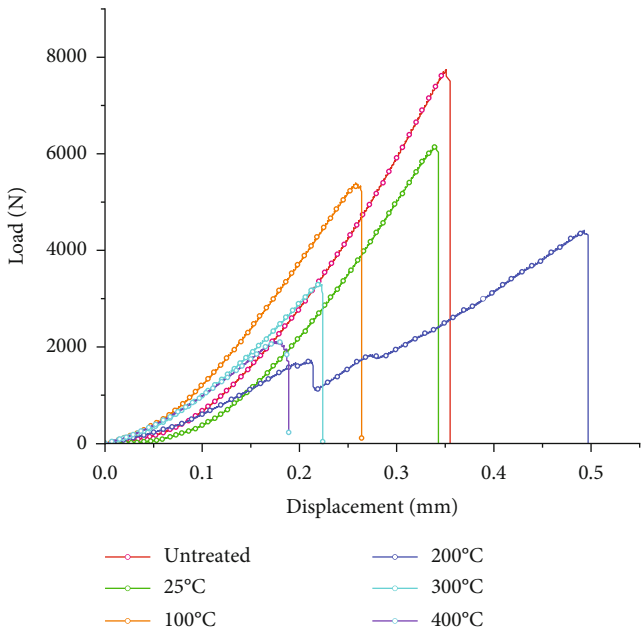

Figure 4: Load-displacement curves.

encompassing heating and liquid nitrogen cooling at temperatures of 25°C, 100°C, 200°C, 300°C, and 400°C. Additionally, untreated specimens without high-temperature heating and liquid nitrogen cooling were included for comparison.

Firstly, we investigated the impact of liquid nitrogen cooling treatment on the load-displacement behavior of granite specimens. During the initial compaction stage at $T_0 = 25 \circ C$, the load-displacement curve of the specimens subjected to liquid nitrogen cooling treatment displayed a comparatively slower rate of change when compared to the untreated specimens. This indicates that the granite specimens after liquid nitrogen cooling treatment experienced larger displacements under smaller loads. After the granite specimens underwent liquid nitrogen cooling treatment, the drastic temperature variation caused the contraction of tiny particles within the granite and the development and extension of preexisting fissures, as well as the formation of new fractures within the rock mass. Additionally, the ones treated with liquid nitrogen cooling exhibited a longer initial compaction stage, further confirming the development of internal fissures within the granite specimens due to the cooling treatment [30].

Moreover, we examined the impact of varying initial temperatures on the load-displacement curve of the granite specimens. During the initial stage, an increase in the initial temperature resulted in a conspicuous alteration in the load variation of the specimen for a given displacement. Based on the graph, it is evident that as the initial temperature T_0 rose from 25 to 200°C, the load-displacement curve exhibited a steeper slope, signifying that the rate of load increase surpassed the rate of displacement growth. Conversely, when the initial temperature T_0 increased from 300 to 400°C, the load-displacement curve gradually flattened, suggesting that the rate of load growth became smaller than the rate of displacement increase. This phenomenon can be attributed to the thermal expansion of the rock particles within a specific range of elevated temperatures. Although there is thermal stress generated during this process, the rock does not reach its strength limit and therefore does not experience failure or microcracks. The result of thermal expansion, to some extent, contributes to an increase in rock density and consequently enhances rock strength. Nevertheless, with escalating temperatures, the thermal stress intensifies considerably, possibly surpassing the rock's strength threshold. Consequently, this leads

to the progression of preexisting cracks and the emergence of novel microcracks within the granite specimen.

During the elastic stage, as the initial temperature T_0 gradually rises, the load-displacement curve maintains a linear relationship. Nevertheless, with increasing temperatures, the initially rising slope of the curve eventually diminishes. This phenomenon can be attributed to the thermal expansion experienced by the rock particles, which enhances the interaction between them, thereby endowing the rock specimen with an elevated capacity to withstand elastic deformation. As the temperature continues to rise, irreversible damage takes place within the granite specimen; however, the load-displacement curve still exhibits a linear relationship. During the crack propagation stage, when the temperature rises within a certain range, the period of crack extension increases, indicating that appropriate heating of the granite specimen improves its ductility. However, when the temperature exceeds a certain threshold and the heating of the specimen continues, the ductility of the specimen deteriorates. This phenomenon can be attributed to the elevated temperature, which leads to the development of interconnected preexisting gaps and the generation of numerous new microcracks within the specimen.

During the crack propagation stage, the granite specimens that have undergone liquid nitrogen cooling treatment exhibit a longer crack propagation period, indicating that the treatment enhances the ductility of the granite specimens. However, in the failure stage, all granite specimens demonstrate brittle failure. As the initial temperature of the granite increases, the rate of decline in peak load also accelerates. It is evident that the greater the temperature difference between the granite and liquid nitrogen, the more severe the thermal damage incurred within the rock, making the granite more prone to deformation failure.

After high-temperature heating and liquid nitrogen cooling treatment, the mechanical properties of the granite significantly decrease, while its ductility is improved to some extent. This indicates that in the actual engineering of liquid nitrogen-assisted fracturing of high-temperature reservoir rocks, liquid nitrogen can significantly reduce the fracturing pressure of reservoir rocks, making it easier for rocks to fracture. In addition, the improvement in ductility makes it less likely for rocks to form a single crack, but rather more likely to form a network of cracks with branches.

3.2. Analysis of Acoustic Emission Characteristics of Granite. In response to abrupt stress changes at defective sites, the structural integrity of materials undergoes deformation and fracture under the influence of external factors such as external forces and temperature. This localized energy release results in the generation of transient elastic waves and audible sounds, a phenomenon known as acoustic emission (AE) [31].

By conducting acoustic emission experiments and analyzing the collected AE signals, the damage characteristics of rocks during the loading process can be obtained. Precise processing of the acquired acoustic wave signals is performed, and then, the rock damage assessment is conducted based on the variations of characteristic parameters. The processing of AE signals mainly involves parameter analysis and waveform analysis [32]. Parameter analysis is the most widely used signal processing method. In the parameter analysis, the monitored signals undergo preprocessing, where they are transformed into characteristic parameters. In the parameter analysis, the monitored signals undergo preprocessing, where they are transformed into characteristic parameters. Subsequently, statistical analysis is conducted based on the variations and relationships among these parameters. In this experiment, ring-down counts and energy counts were selected for single-parameter analysis.

To obtain acoustic emission (AE) data for different high-temperature granite subjected to cooling during three-point bending tests, a real-time AE acquisition system was utilized to capture emitted signals during the failure process of the granite. The corresponding information regarding AE ring-down counts and cumulative ring-down counts at various temperatures during the three-point bending tests is displayed in Figure 5. Additionally, Figure 6 presents a line graph depicting the correlation between cumulative ring-down counts and temperature for the two distinct temperature groups.

From Figure 5, it can be observed that the four stages of granite sample failure in the three-point bending test are closely correlated with the variation in ring-down counts of acoustic emissions. During the initial compaction stage, when the sample is subjected to relatively low loads, the rate of ring-down counts is small, and the signals remain stable. Only a brief period of active signals was observed in the temperature group $T_0 = 25 \circ \mathrm{C}$. The cumulative ring-down count curve shows a small increment and remains relatively constant. The primary source of acoustic emission signals during this stage is the relative sliding friction between internal rock particles.

During the elastic stage, the ring-down count signals remain relatively inactive. However, in contrast to the compaction stage, the events in this particular stage exhibit a higher magnitude, resulting in a gradual increase in cumulative ring-down counts and an elevated slope in the curve. This can be attributed to the occurrence of microcracks, relative sliding, and slight self-structural adjustments within the granite in order to achieve optimal load-bearing conditions. Under certain temperature conditions, the cumulative ring-down counts of some samples even reach magnitudes in the thousands, accompanied by a sudden change in cumulative ring-down counts. This phenomenon is attributed to the cooling effect of liquid nitrogen on the granite, which reduces its strength and deformation resistance.

During the crack propagation stage, also known as the yielding stage, the ring-down count suddenly increases as the load gradually increases. As the signals become active, multiple spikes emerge, resulting in a rapid surge of cumulative ring-down counts characterized by a steep slope in the curve. In this stage, the rock begins to generate a large number of microcracks and experiences partial fracturing. Simultaneously, these microcracks further develop and connect, eventually forming macroscopic cracks. During the failure stage, the ring-down count experiences a sharp increase, reaching its maximum value at the instant when the load-displacement curve drops. The cumulative ring-down count exhibits a significant increase during this moment. Upon the

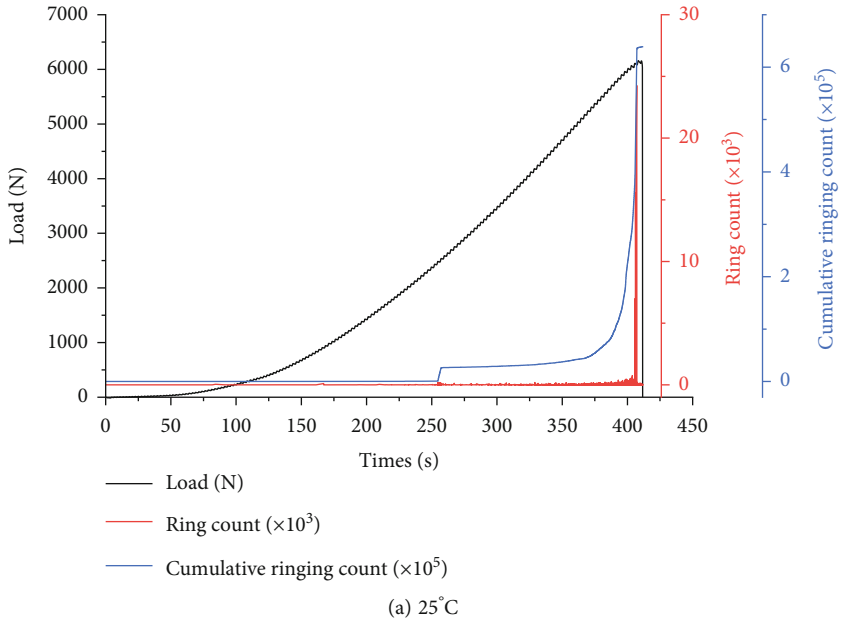

(a) 25°C

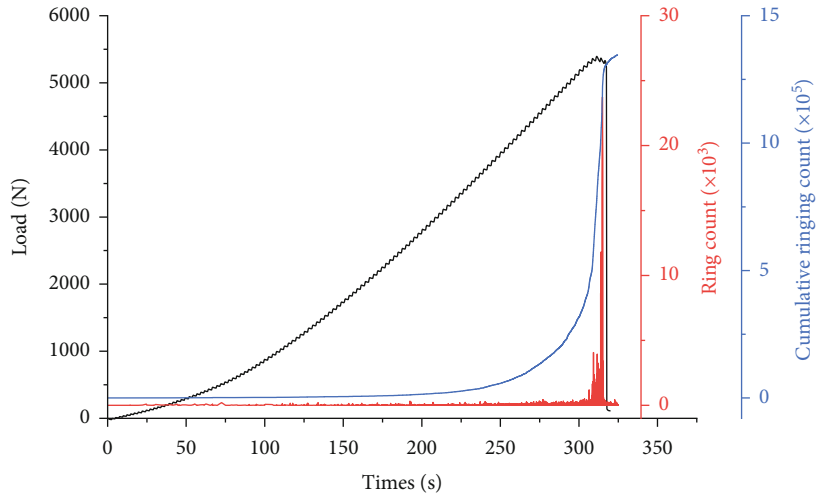

(b) 100°C

Figure 5: Continued.

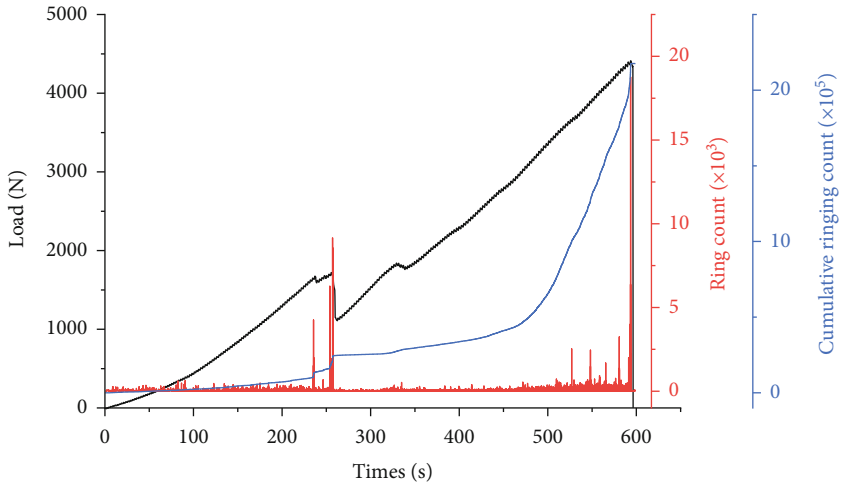

Load (N)
Ring count ($\times 10^3$)
Cumulative ringing count ($\times 10^5$)

(c) 200°C

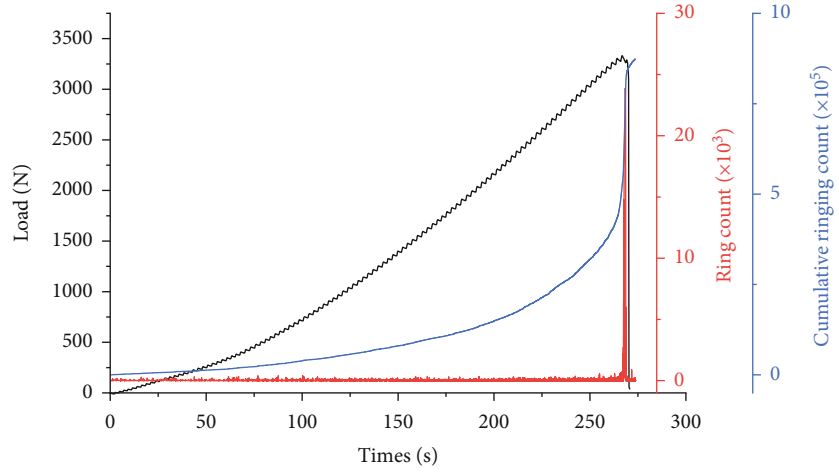

Load (N)
Ring count ($\times 10^3$)
Cumulative ringing count ($\times 10^5$)

(d) 300°C

Figure 5: Continued.

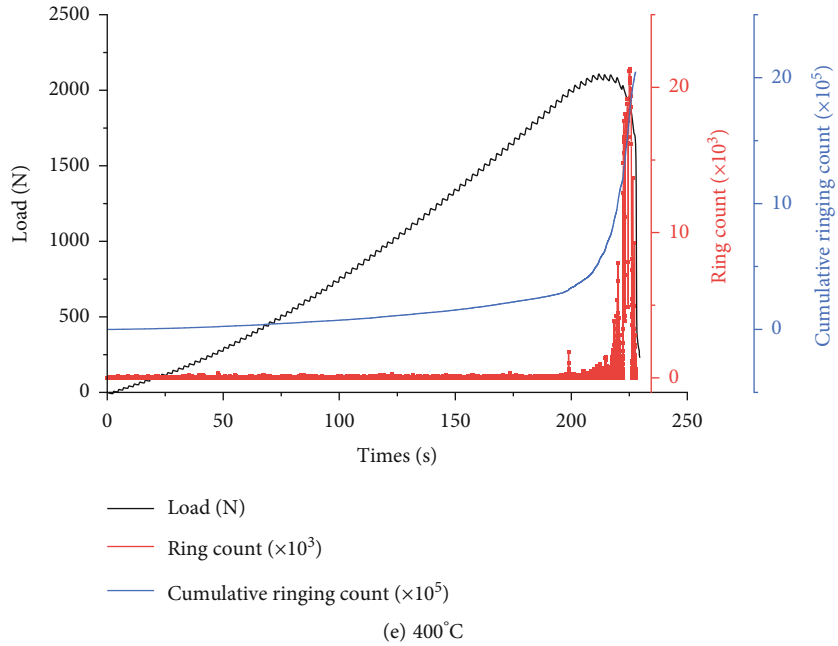

Figure 5: The variation pattern of ring-down counts during the three-point bending test on granite.

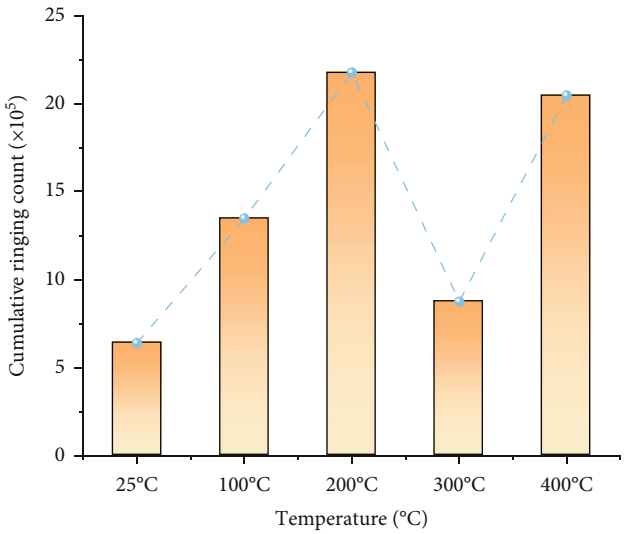

Figure 6: The relationship between cumulative ring-down counts and temperature in the three-point bending experiment.

complete loss of load-bearing capacity and failure of the rock specimen, the ring-down count exhibits a rapid decline and ultimately diminishes as the stress within the rock mass is released.

Acoustic emission counts represent the initiation and development of microcracks within the specimen, and a higher count indicates a greater number of microcracks inside the granite. By comparing the acoustic emission counts of granite specimens at different initial temperatures, it can be observed that higher initial temperatures result in a higher count of acoustic emissions during granite fracturing. This suggests that a larger temperature difference between liquid nitrogen and high-temperature granite leads to more severe internal damage within the granite, resulting in a greater number of microcracks and more complex fractures during fracturing.

As shown in Figure 6, the cumulative decrement counts exhibit significant fluctuations with changes in temperature. Within a certain temperature range, the cumulative decrement counts gradually increase with rising temperature, then decrease and enter a repetitive oscillation stage characterized by subsequent increases and decreases. This indicates that there is no absolute linear relationship between the cumulative counts of granite samples and their initial temperatures, as factors such as the initial damage and uneven stress distribution within the granite may affect its final cumulative count. Therefore, in future experimental studies, the relationship between acoustic emission cumulative counts and initial temperature of granite can be explored further by increasing the sample size.

Figure 7 displays the pertinent information pertaining to acoustic emission energy and cumulative energy counts during the three-point bending tests conducted on granite at various temperatures in this investigation. According to Figure 7, energy counts serve as an indicator reflecting the damage characteristics during the loading process of rocks and can be analyzed based on four stages. In the initial compaction stage of granite, the internal microcracks gradually close, resulting in weak energy count signals at a magnitude of only single digits. The curve of cumulative energy counts remains relatively unchanged during this stage, with a slope that approaches horizontal.

During the elastic stage, although there is a slight increase in energy counts, they remain relatively small. Towards the later stage of this compaction phase, the cumulative energy count curve demonstrates a gradual upward trend. During the yielding stage, energy counts start to increase rapidly, and the abrupt points on the cumulative energy count curve can be clearly observed, with the

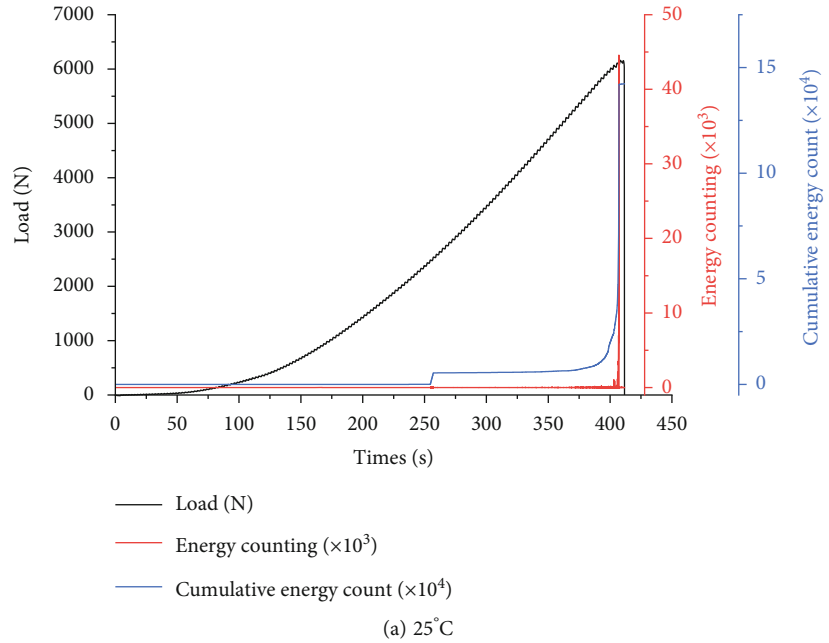

(a) 25°C

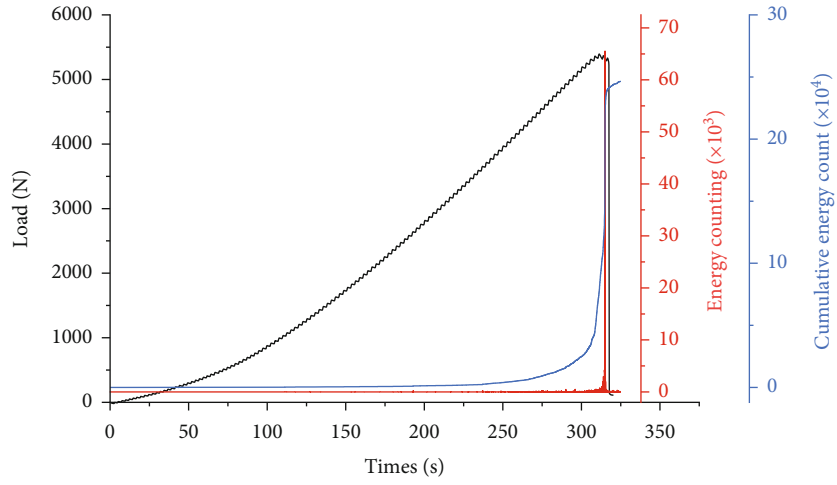

(b) 100°C

Figure 7: Continued.

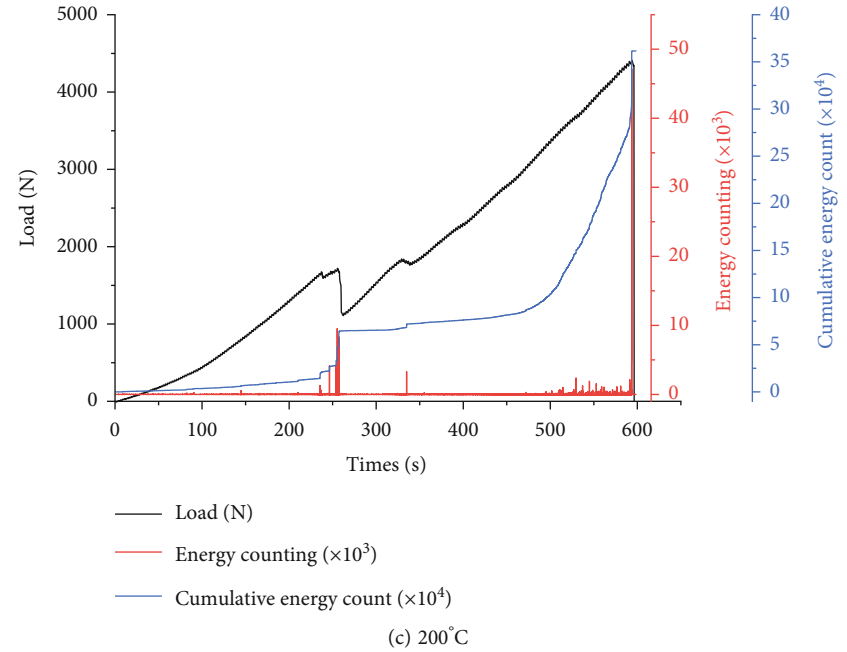

(c) 200°C

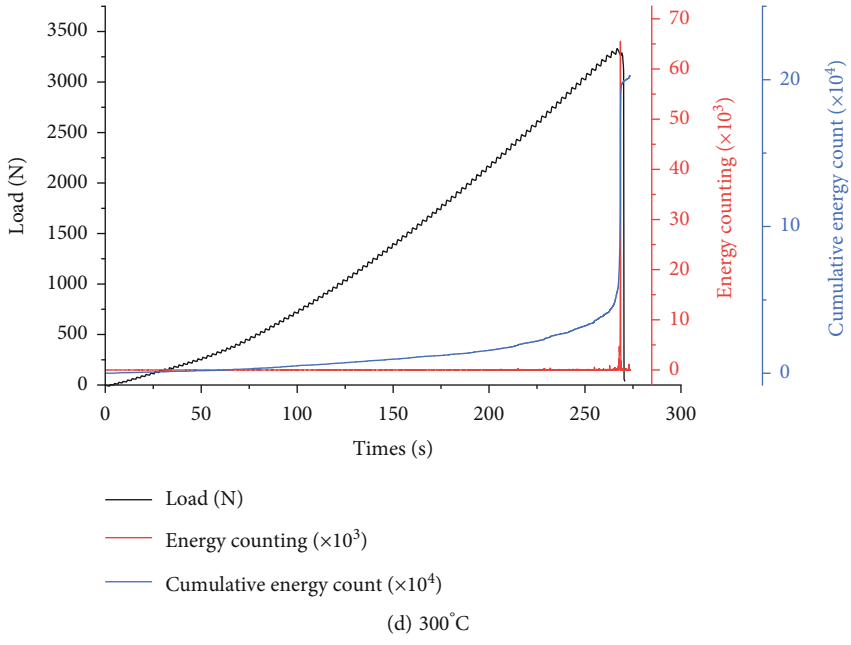

(d) 300°C

Figure 7: Continued.

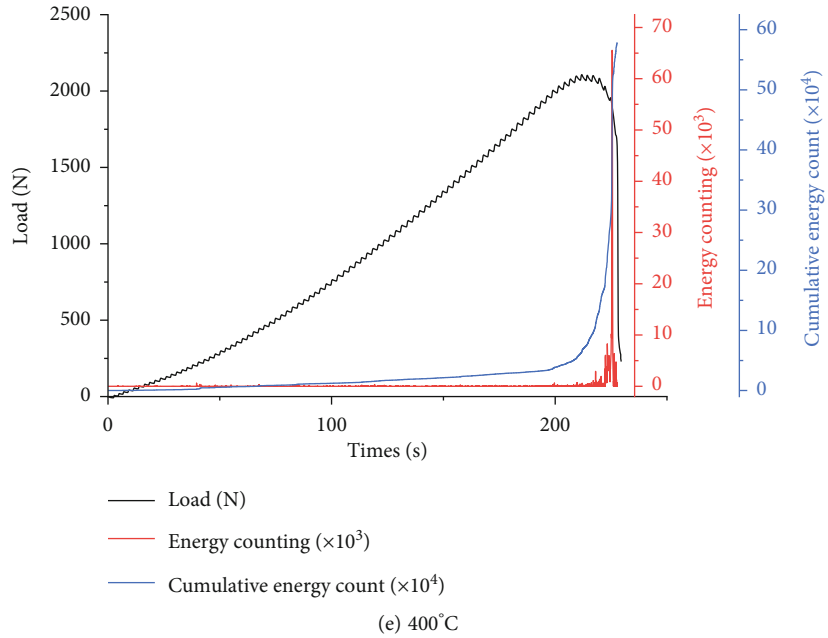

Figure 7: The variation pattern of energy counts in the three-point bending tests of granite samples.

cumulative values rising rapidly. This stage marks the occurrence of rock fracturing, characterized by the generation and propagation of numerous microcracks that eventually connect to form macroscopic fractures. Across different temperatures, the prolonged loading time leads to distinct transitions in the cumulative energy count curve. The magnitude of acoustic emission energy counts is influenced by two key factors: the number of instantaneous acoustic emission events and the amount of strain energy released by the rock during the formation of microcracks. Moreover, the release of strain energy through microcracks in the rock is closely associated with the interactions among mineral particles. It is hypothesized that in the case of granite treated with liquid nitrogen cooling, thermal stress disrupts the connections between mineral particles, making relatively stable microcracks more prone to connectivity and subsequent crack propagation damage. Elevated initial temperatures and larger temperature differentials exacerbate the destabilizing impact of liquid nitrogen cooling on the interparticle connections within the mineral matrix. Consequently, this leads to a shorter duration of stable crack propagation and an extended duration of unstable crack propagation within the granite specimen.

During the failure stage, when the load reaches its peak, the energy counts also reach their peak, and the changes in cumulative energy counts are highly noticeable. At this point, the specimen undergoes complete loss of its load-bearing capacity, resulting in the generation of a fracture surface. From an overall perspective, the cumulative energy count curve of the specimen exhibits significant fluctuations. When the initial temperatures are 25°C, 100°C, 200°C, 300°C, and 400°C, respectively, the cumulative energy counts for the temperature group with liquid nitrogen cooling are 333617, 202778, 195877, 170834, and 163797. With an increase in the initial temperature, there is a gradual decrease in the cumulative energy counts. This observation suggests that the application of liquid nitrogen cooling treatment can effectively mitigate the energy required for granite failure, particularly at higher temperatures.

3.3. Energy Analysis of Granite. To delve deeper into the impact of various temperature treatments on granite, an examination was conducted to ascertain the correlation between the applied load and the energy exhibited by the granite. This investigation relied on the analysis of load-displacement curves, as depicted in Figures 8 and 9.

From Figures 8 and 9, it can be observed that the variation of peak energy with load is similar to the variation of peak load with displacement. Furthermore, the load-energy graph bears a striking resemblance to the displacement-load graph, with both exhibiting distinguishable stages that can be broadly categorized as follows: initial densification, elastic response, yield point, and ultimate failure. The specific reasons for this similarity have been discussed earlier in the analysis of load-displacement graphs. After being subjected to high-temperature heating and liquid nitrogen cooling treatment, the peak load of granite is reduced, while its ductility characteristics are improved. Additionally, the higher the initial temperature of the granite, the more severe the cold impact effect caused by liquid nitrogen. Under the action of external loads, the total energy absorbed by the rock gradually increases [33]. However, due to the thermal stress between liquid nitrogen and high-temperature rock, thermal cracking occurs inside the granite, thereby reducing its mechanical bearing capacity and subsequently decreasing the absorbed energy. In addition, the cold impact effect of liquid nitrogen also weakens the granite's ability to resist deformation failure, resulting in a decrease in the initiation pressure of the granite.

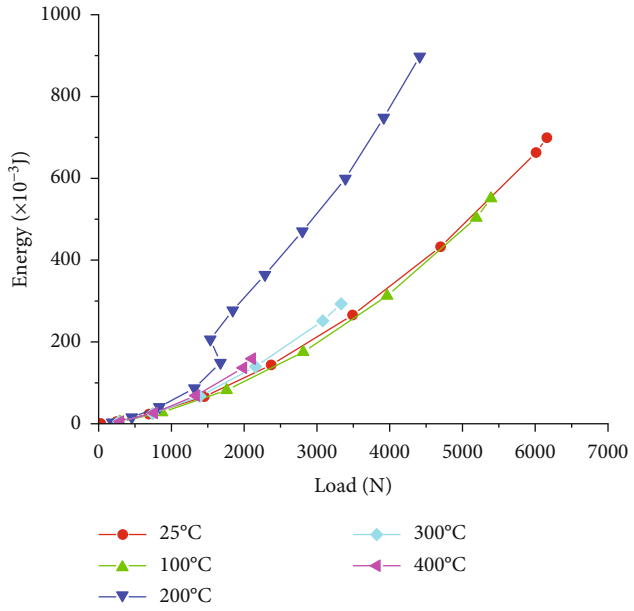

Figure 8: Load-energy diagram of granite.

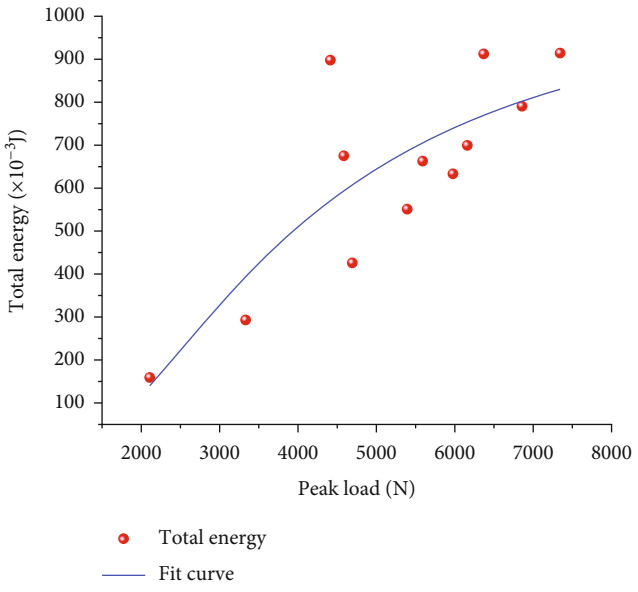

Figure 9: Relationship between peak load and total energy of granite.

4. Analysis of Granite Wave Velocity

In practical engineering applications of rock mechanics, ultrasound velocity serves as an important parameter, which is primarily influenced by factors such as the type of propagation medium and porosity within the rock mass [34–36]. The propagation velocity of ultrasound differs among various media. When ultrasound propagates within rocks, it encounters scattering or waveform transformations due to the presence of fractures and fissures within the rock mass. Therefore, by detecting variations in wave velocity, it is possible to study the development of fractures and structural changes within the rock mass based on this regularity. Ultrasound waves can be classified into three primary types, namely, longitudinal waves, transverse waves, and torsional waves. This classification is based on the direction of wave propagation and the vibration direction of particles within the medium. Longitudinal waves propagate due to volume changes caused by external loads acting on the rock mass, and they can propagate in gas, liquid, and solid media, but with varying propagation velocities in different mediums. In this section, the experimental measurements focus on the P-wave velocity of granite. Figure 10 illustrates the variations in granite P-wave velocity at different temperatures.

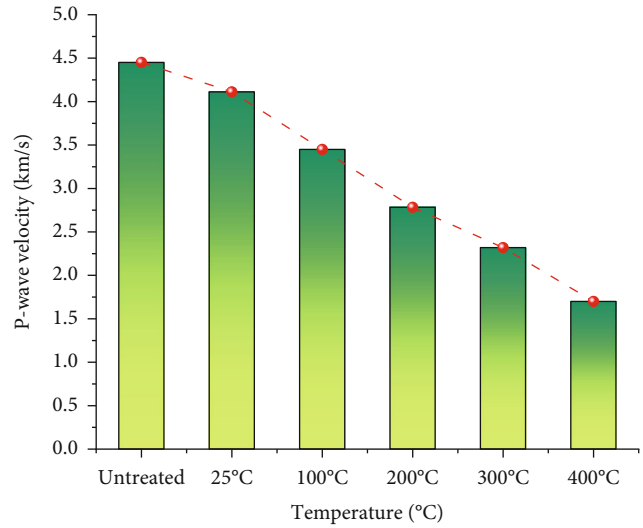

Figure 10: P-wave velocity of granite at different temperatures.

In Figure 10, it is evident that the internal P-wave velocity in the granite specimens diminishes gradually as the temperature ascends. Notably, at an initial temperature of 25°C, the liquid nitrogen-cooled group displays a substantial decrease in P-wave velocity compared to the noncooled group. This phenomenon can be attributed to the transformation of the granite's properties from brittle to ductile after being treated with liquid nitrogen. Consequently, this treatment leads to an enlargement of fractures and pores within the rock mass, hindering the smooth propagation of acoustic wave signals due to the obstructions caused by these features. Additionally, these pores and fractures tend to absorb high-frequency waves. As a result of undergoing liquid nitrogen cooling treatment, a substantial decrease in the P-wave velocity of the granite is observed.

As the initial temperature rises, the decline in P-wave velocity within the granite specimens becomes increasingly prominent. This study postulates that the primary reason for this phenomenon lies in the cooling process of the granite, whereby it is subjected to high-temperature heating followed by rapid cooling with liquid nitrogen. This cooling treatment generates numerous new microcracks within the granite, which act as hindrances to the propagation of acoustic waves. Consequently, the wave velocity undergoes significant changes. This discovery provides additional confirmation regarding the efficacy of employing observed

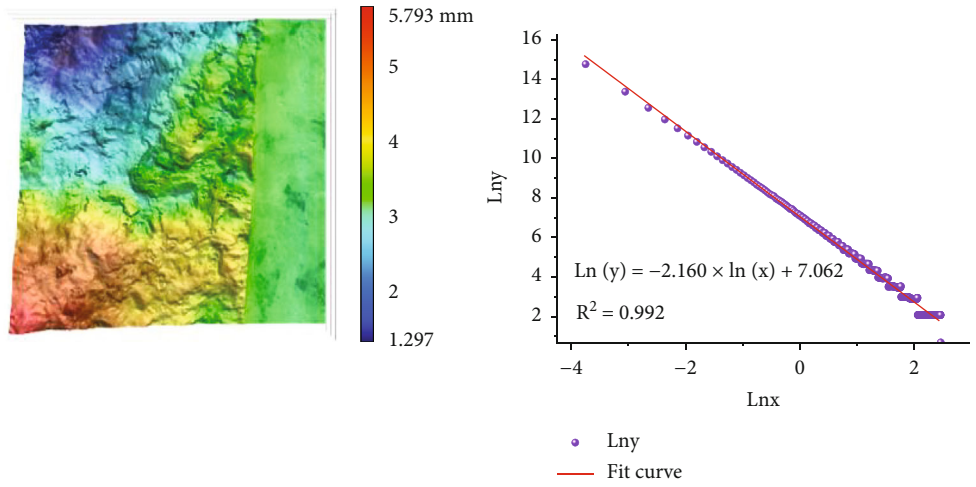

(a) 25°C

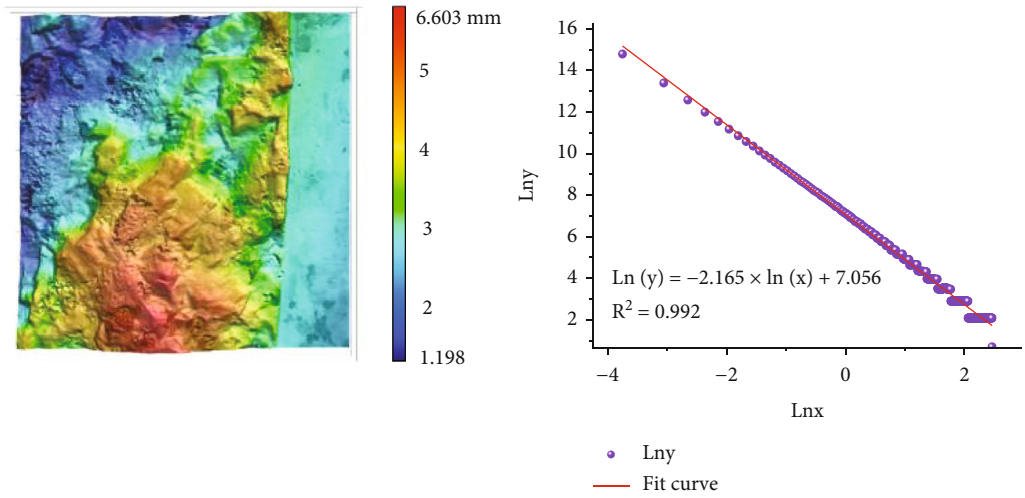

(b) 100°C

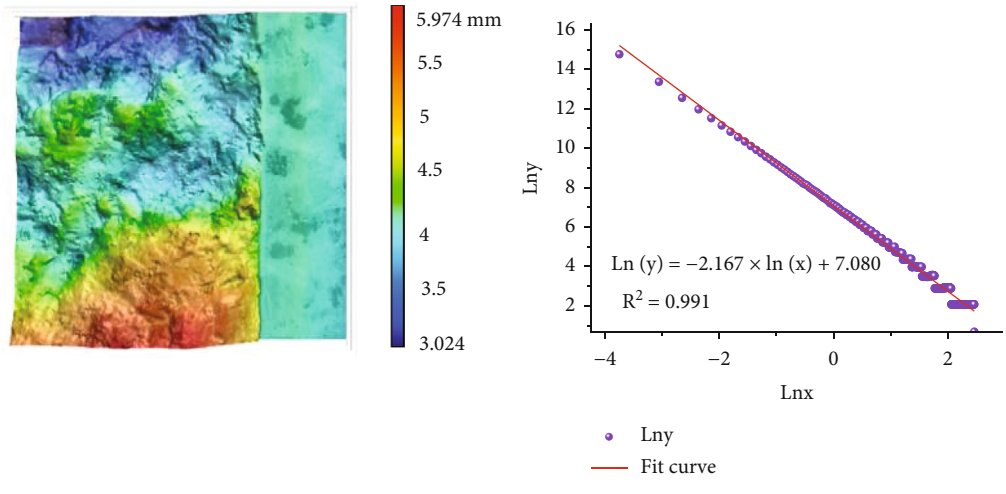

(c) 200°C

Figure 11: Continued.

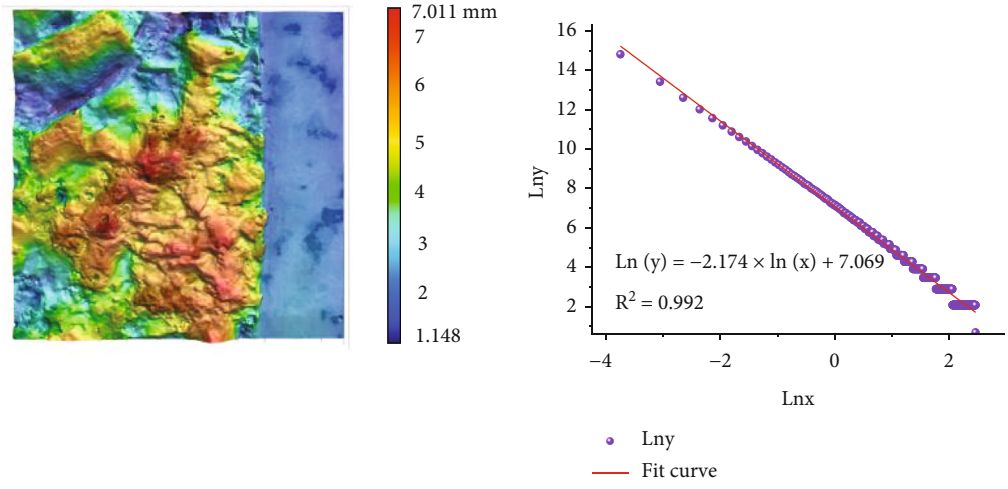

(d) 300°C

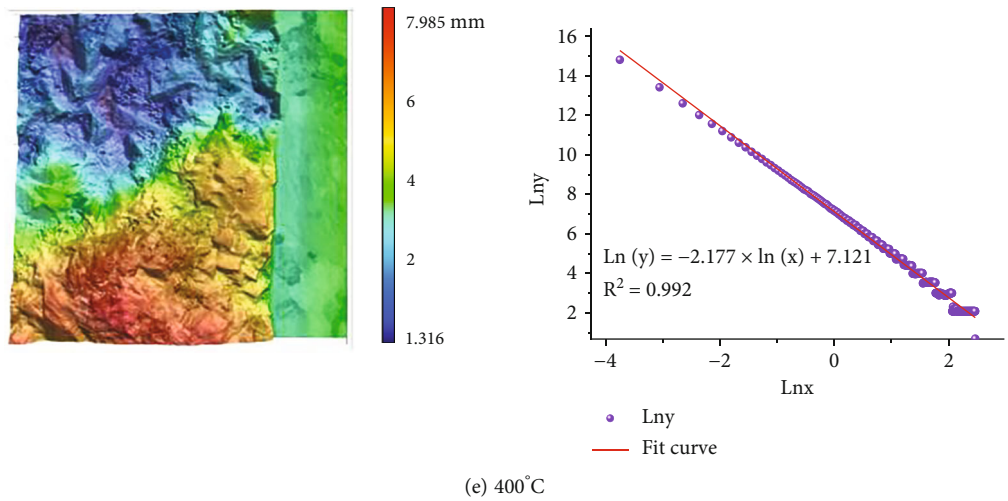

(e) 400°C

Figure 11: The cross-sections of granite samples at different temperatures.

fluctuations in P-wave velocity as a means of evaluating the degree of crack development within rock masses.

Variations in the initial temperature of rock samples generate thermal stress within the rock mass as a consequence of the temperature discrepancies between the surface and interior of the rock. In the presence of substantial temperature disparities, the rock's interior is subjected to elevated thermal stress, consequently leading to the formation of microcracks. Simultaneously, due to the effects of high temperatures, the rock's inherent strength diminishes, giving rise to interconnected fractures within the interior. As a result, the continuous formation of new microcracks and the propagation of existing cracks contribute to the escalation in both the quantity and size of cracks within the rock mass. This progressive development of internal cracks induces microscopic damage within the rock mass, thus characterizing the thermal damage process.

5. Scanning Section Study of Granite

After subjecting granite to high-temperature heating, it was cooled using liquid nitrogen, followed by the application of external loads. As the load gradually increased, the granite inevitably experienced cracking once the load reached its peak limit. In addition to the visibly obvious surface cracks, the cracking of granite also gave rise to microcracks that are difficult to observe with the naked eye. Based on this, the present experiment utilized a three-dimensional cross-sectional scanning device, namely, the VR-5000 series 3D profilometer, to scan the treated granite samples. By observing and analyzing their surface morphology, the impact of different temperatures on the degree of damage inflicted upon the granite specimens was investigated.

5.1. Analysis of Surface Characteristics of Granite. To investigate the surface characteristics of fractured granite, a thorough analysis was performed utilizing an advanced three-dimensional scanning device. Figure 11 presents the surface characteristics of granite under different temperature treatments, while Figure 12 illustrates the values of the fractal dimension, D, at varying temperatures.

Based on Figure 11, it can be observed that the fitting accuracy exceeds 0.99, indicating that the fractured surfaces exhibit excellent fractal characteristics. Additionally, Figure 12

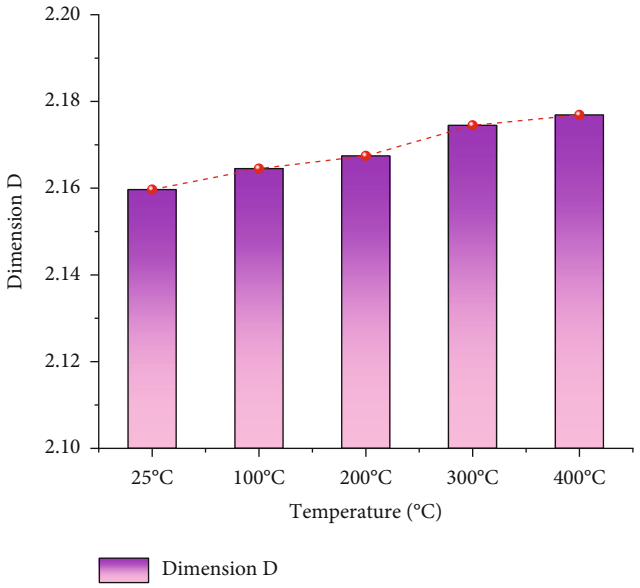

Figure 12: Fractal dimension of granite samples at different temperatures.

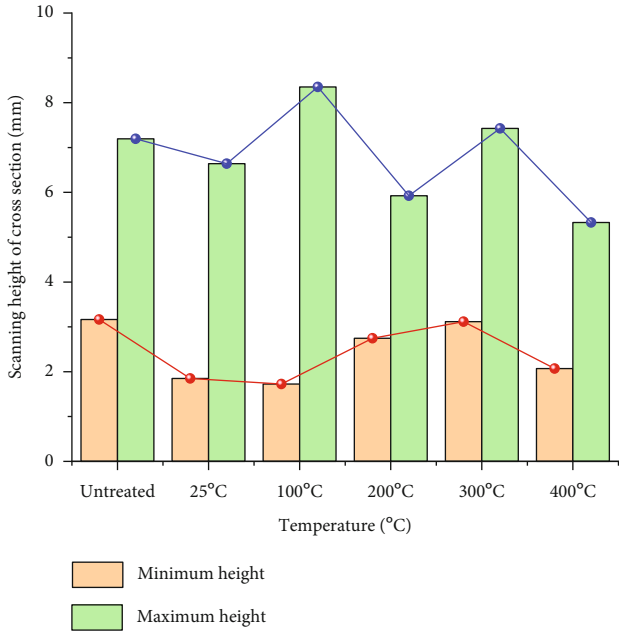

Figure 13: Maximum and minimum heights of granite samples at different temperatures.

demonstrates that the fractal dimensions of the granite samples' fractured surfaces vary significantly under different temperature conditions. This can be attributed to the positive correlation between fractal dimension and roughness; as the degree of fracture increases, so does the surface roughness, resulting in larger fractal dimensions. The increased roughness is manifested by enhanced irregularities in the fracture morphology. Specifically, the height difference between the highest and lowest points on the fractured surface becomes more pronounced, leading to an uneven appearance when scanned using our imaging device, as depicted in Figure 13. The augmented roughness can be attributed to not only the increase in porosity caused by the cooling effect of liquid nitrogen but also the external loading, which facilitates further development of internal cracks and crack propagation within the granite samples, thereby enhancing the complexity of the fracture surface morphology. By comparing the fracture surfaces of granite at different initial temperatures, we can observe that as the initial temperature increases, the fracture surface of granite becomes rougher and is accompanied by the appearance of numerous micropores. This is due to larger temperature gradients leading to more severe damage. Under external loads, internal microcracks in granite connect with each other and traverse the entire structure, resulting in more complex fracture surfaces, while the permeability of granite is also increased.

The advantage of liquid nitrogen fracturing technology lies in its ability to reduce the initiation pressure of hot dry rocks and guide the formation of a large-scale three-dimensional fracture network within them. Based on the analysis above, it can be concluded that an increase in the roughness of granite fracture surfaces indicates the formation of a more complex network of cracks during the failure and destruction process of granite. As the initial temperature of the granite rises, the cold impact effect of liquid nitrogen becomes stronger. This has been confirmed in the numerical simulations and experimental studies conducted by Xue et al. [37]. Additionally, by increasing the number of liquid nitrogen treatments, the formation of microcrack networks in high-temperature granite can also be promoted [38]. Therefore, in practical engineering applications, suitable methods should be chosen based on ground stress and project costs in order to achieve the goal of maximizing economic benefits.

5.2. Analysis of Fracture Toughness in High-Temperature Granite. Fracture toughness, as a physical-mechanical property of rocks, serves as an indicator of their ability to withstand crack propagation. Based on the morphological characteristics of fracture surfaces, they can generally be classified into three types: opening mode, sliding mode, and tearing mode. The occurrence of the tearing mode is frequently observed in rock fracture surfaces. The evaluation of rock fracture toughness can be accomplished through a three-point bending test, wherein the calculation formulas are presented in [39, 40]

$$S' = \frac{S}{2R}, \tag{1}$$

$$a' = \frac{a}{R} \tag{2}$$

$$Y = -1.297 + 9.516S' - \left(0.47 + 16.457S'\right)a' + \left(1.071 + 34.401S'\right)a'^2, \tag{3}$$

$$K_{IC} = \frac{P_{max}\sqrt{\pi a}}{2RB}Y. \tag{4}$$

In this equation, S represents the distance between the support points, a denotes the crack depth with a value of

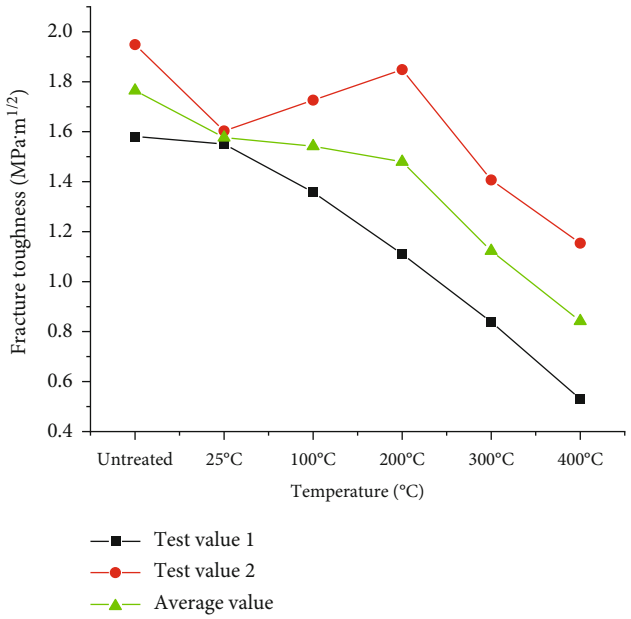

FIGURE 14: Change of fracture toughness of granite samples at different temperatures.

14 mm, R signifies the radius with a value of 38 mm, B stands for the width with a value of 30 mm, K_{IC} represents the fracture toughness, and Y represents the factor.

According to the ISRM recommendations for type I quasi-static fracture toughness testing of rock-like materials, the spacing between support points (S) and the specimen diameter ($2R$) should satisfy a certain ratio $0.5 \le S' \le 0.8$. In this experiment, the chosen ratio is 0.5, which means $S = 38$ mm [41].

According to the given values, substituting them into Equation (1) and Equation (2) yields $S' = 0.5$ and $a' = 0.368$, respectively. Subsequently, by substituting these values into Equation (3), we can determine $Y = 2.734$.

By integrating the aforementioned values with the maximum load values of the specimens at varying temperatures, the fracture toughness of each specimen under different conditions can be determined, as shown in Figure 14.

Figure 14 reveals a significant reduction in the fracture toughness of granite specimens with a gradual increase in temperature. This decline can be attributed to a consistent relationship between the internal wave velocity changes within the specimens at various temperatures and the initial temperature, as discussed earlier. As the temperature further increases, irreversible damage occurs in the rock, causing the development and connection of preexisting cracks within the specimens, as well as the generation of a significant number of new cracks. Consequently, the strength of the rock diminishes.

6. Conclusion

This research focuses on granite and systematically investigates the damage mechanism of liquid nitrogen-induced crack propagation in high-temperature rocks through different temperature heating and liquid nitrogen cooling treatments. Various methods such as three-point bending tests, acoustic emission detection, ultrasonic flaw detection, and three-dimensional section scanning experiments were used to analyze the cold impact effect of liquid nitrogen on high-temperature granite. The main research findings are as follows:

(1) After undergoing high-temperature heating and liquid nitrogen cooling treatments, the peak load of granite decreases. This is because high-temperature heating causes the expansion and damage of internal microcracks in the rock, while liquid nitrogen cooling leads to excessive development of internal cracks and enhanced connectivity of small cracks in granite, further weakening its deformation resistance. However, despite the decrease in peak load, the liquid nitrogen-cooled granite exhibits better ductility

(2) Analysis of acoustic emission signals and fracture surface roughness shows that the number of observed microcracks in liquid nitrogen-cooled granite increases with the rise of the initial temperature. The phenomenon of small rock particles peeling off from the surface becomes more pronounced, resulting in extremely rough morphology and numerous micropores

(3) During the liquid nitrogen cooling process, granite is subjected to rapid temperature changes and thermal stresses. This sudden cooling results in significant temperature gradients inside and on the surface of granite. Under high-temperature conditions, stress concentration and increased deformation accelerate the expansion of microcracks, leading to more severe and faster damage and failure processes

In summary, this study involved the liquid nitrogen cooling treatment of granite at different initial temperatures and extensively investigated the mechanical properties, acoustic emission characteristics, and roughness of fracture surfaces of granite. The research results indicate that the low-temperature effect of liquid nitrogen has a significant fracturing impact on high-temperature granite. Furthermore, when using liquid nitrogen for fracturing assistance, it is important to develop reasonable construction plans based on actual site conditions, reservoir rock types, and in situ stress factors. This will help to improve engineering efficiency and successfully implement liquid nitrogen fracturing technology.

Data Availability

The data used to support the findings of this study are included within the article.

Conflicts of Interest

The authors declare that there are no conflicts of interest.

Acknowledgments

The authors are grateful to the financial support from the National Natural Science Foundation of China (52204112 and 42007264), the Key Research and Development Program of Shaanxi Province, China (2022ZDLSF07-06 and 2023-YBSF-369), the Natural Science Basic Research Program of Shaanxi (2022JM-216 and 2022JC-LHJJ-08), and the Scientific Research Program Funded by Shaanxi Provincial Education Department (No. 22JK0480).

References

[1] D. Chang, J. Zuo, Z. Zhao, G. Zillante, X. Gan, and V. Soebarto, "Evolving theories of sustainability and firms: History, future directions and implications for renewable energy research," *Renewable and Sustainable Energy Reviews*, vol. 72, pp. 48–56, 2017.

[2] J. Liu, Y. Xue, Y. Fu, K. Yao, and J. Liu, "Numerical investigation on microwave-thermal recovery of shale gas based on a fully coupled electromagnetic, heat transfer, and multiphase flow model," *Energy*, vol. 263, article 126090, 2023.

[3] T. Li, W. Zhao, R. Liu, J. Y. Han, P. Jia, and C. Cheng, "Visualized direct shear test of the interface between gravelly sand and concrete pipe," *Canadian Geotechnical Journal*, 2023.

[4] W. Wang, J. Wu, and S. Shi, "Probe a new energy-hot dry rock," *Exploration Engineering (Rock & Soil Drilling and Tunneling)*, vol. 47, no. 3, pp. 88–93, 2020.

[5] L. I. Ting-liang, C. A. O. Wen-jiong, W. A. N. G. Yi-wei, G. U. O. Jian, and J. I. A. N. G. Fang-ming, "Laboratory study on hydraulic fracturing and acoustic emission monitoring of enhanced geothermal system," *Advances in New & Renewable Energy*, vol. 7, no. 3, 2019.

[6] G. U. O. Qinghai, H. E. Tong, Z. H. U. A. N. G. Yaqin, L. U. O. Jin, and Z. H. A. N. G. Canhai, "Expansion of fracture network in granites via chemical stimulation: a laboratory study," *Earth Science Frontiers*, vol. 27, no. 1, p. 159, 2020.

[7] M. Brehme, G. Blöcher, S. Regenspurg et al., "Approach to develop a soft stimulation concept to overcome formation damage–a case study at Klaipeda, Lithuania," in *Proceedings of the 42nd Workshop on Geothermal Reservoir Engineering*, Stanford, California, February 2017.

[8] J. Han, J. Wang, D. Jia et al., "Construction technologies and mechanical effects of the pipe-jacking crossing anchor-cable group in soft stratum," *Frontiers in Earth Science*, vol. 10, article 1019801, 2023.

[9] K. Breede, K. Dzebisashvili, X. Liu, and G. Falcone, "A systematic review of enhanced (or engineered) geothermal systems: past, present and future," *Geothermal Energy*, vol. 1, no. 1, pp. 1–27, 2013.

[10] X. X. Wang, N. Y. Wu, Z. Su, and Y. C. Zeng, "Progress of the enhanced geothermal systems (EGS) development technology," *Progress in Geophysics*, vol. 27, no. 1, pp. 355–362, 2012.

[11] E. Barbier, "Geothermal energy technology and current status: an overview," *Renewable and Sustainable Energy Reviews*, vol. 6, no. 1-2, pp. 3–65, 2002.

[12] J. Han, J. Wang, C. Cheng et al., "Mechanical response and parametric analysis of a deep excavation structure overlying an existing subway station: a case study of the Beijing subway station expansion," *Frontiers in Earth Science*, vol. 10, p. 1079837, 2023.

[13] S. Kelkar, G. WoldeGabriel, and K. Rehfeldt, "Lessons learned from the pioneering hot dry rock project at Fenton Hill, USA," *Geothermics*, vol. 63, pp. 5–14, 2016.

[14] S. Zhang, Z. Huang, H. Zhang et al., "Experimental study of thermal-crack characteristics on hot dry rock impacted by liquid nitrogen jet," *Geothermics*, vol. 76, pp. 253–260, 2018.

[15] S. R. Grundmann, G. D. Rodvelt, G. A. Dials, and R. E. Allen, "Cryogenic nitrogen as a hydraulic fracturing fluid in the Devonian shale," in *Paper presented at the SPE Eastern Regional Meeting*, p. SPE-51067, Pittsburgh, Pennsylvania, November 1998.

[16] S. Coetzee, H. W. J. P. Neomagus, J. R. Bunt, C. A. Strydom, and H. H. Schobert, "The transient swelling behaviour of large (−20 + 16 mm) South African coal particles during low-temperature devolatilisation," *Fuel*, vol. 136, pp. 79–88, 2014.

[17] B. W. McDaniel, S. R. Grundmann, W. D. Kendrick, D. R. Wilson, and S. W. Jordan, "Field applications of cryogenic nitrogen as a hydraulic fracturing fluid," in *Paper presented at the SPE Annual Technical Conference and Exhibition*, p. SPE-38623, San Antonio, Texas, October 1997.

[18] S. Rassenfoss, "In search of the waterless fracture," *Journal of Petroleum Technology*, vol. 65, no. 6, pp. 46–54, 2013.

[19] M. Cha, X. Yin, T. Kneafsey et al., "Cryogenic fracturing for reservoir stimulation–laboratory studies," *Journal of Petroleum Science and Engineering*, vol. 124, pp. 436–450, 2014.

[20] C. Cai, F. Gao, and Y. Yang, "The effect of liquid nitrogen cooling on coal cracking and mechanical properties," *Energy Exploration & Exploitation*, vol. 36, no. 6, pp. 1609–1628, 2018.

[21] Y. Lai, C. Zhai, Y. Sun et al., "Study on damage characteristics of hot dry rock by liquid nitrogen cyclic cold shocks based on ultrasonic testing," *Energy & Fuels*, vol. 37, no. 21, pp. 16573–16587, 2023.

[22] Z. Li, H. Xu, and C. Zhang, "Liquid nitrogen gasification fracturing technology for shale gas development," *Journal of Petroleum Science and Engineering*, vol. 138, pp. 253–256, 2016.

[23] C. Zhang, L. Weilong, W. Xizhao, W. A. N. G. Laigui, and L. I. Hewan, "Research of fracturing mechanism of coal subjected to liquid nitrogen cooling," *Journal of Hebei University of Science & Technology*, vol. 36, no. 4, 2015.

[24] C. Zhang, X. Guo, and W. Li, "Study on influence of liquid nitrogen infiltration to saturated water coal fracture expanded," *Coal Science and Technology*, vol. 44, no. 6, pp. 99–105, 2016.

[25] S. Wang, S. Su, D. Wang et al., "Experimental study on fracture characteristics of coal due to liquid nitrogen fracturing," *Geomechanics for Energy and the Environment*, vol. 33, article 100438, 2023.

[26] C. Li, H. Yao, C. Xin, H. Li, J. Guan, and Y. Liu, "Changes in pore structure and permeability of middle–high rank coal subjected to liquid nitrogen freeze–thaw," *Energy & Fuels*, vol. 35, no. 1, pp. 226–236, 2021.

[27] I. Khurshid, E. W. AlShalabi, H. al-Attar, and A. K. al-Neaimi, "Analysis of formation damage and fracture choking in hydraulically induced fractured reservoirs due to asphaltene deposition," *Journal of Petroleum Exploration and Production Technology*, vol. 10, no. 8, pp. 3377–3387, 2020.

[28] L. Gong, D. Han, Z. Chen et al., "Research status and development trend of key technologies for enhanced geothermal systems," *Natural Gas Industry B*, vol. 10, no. 2, pp. 140–164, 2023.

[29] M. D. Kuruppu, Y. Obara, M. R. Ayatollahi, K. P. Chong, and T. Funatsu, "ISRM-suggested method for determining the mode I static fracture toughness using semi-circular bend specimen," *Rock Mechanics and Rock Engineering*, vol. 47, no. 1, pp. 267–274, 2014.

[30] L. Deng, X. Li, Y. Wu et al., "Influence of cooling speed on the physical and mechanical properties of granite in geothermal-related engineering," *Deep Underground Science and Engineering*, vol. 1, no. 1, pp. 40–57, 2022.

[31] H. R. Hardy, "Applications of acoustic emission techniques to rock and rock structures: a state-of-the-art review," *Acoustic Emissions in Geotechnical Engineering Practice, STP*, vol. 750, pp. 4–92, 1981.

[32] A. Terchi and Y. H. J. Au, "Acoustic emission signal processing," *Measurement and Control*, vol. 34, no. 8, pp. 240–244, 2001.

[33] S. Luo and F. Gong, "Evaluation of rockburst proneness considering specimen shape by storable elastic strain energy," *Deep Underground Science and Engineering*, vol. 1, no. 2, pp. 116–130, 2022.

[34] D. Zhao, S. Zhang, Y. Zhao, and M. Wang, "Experimental study on damage characteristics of granite under ultrasonic vibration load based on infrared thermography," *Environmental Earth Sciences*, vol. 78, no. 14, pp. 1–12, 2019.

[35] M. Zhao and R. Xu, "The rock damage and strength study based on ultrasonic velocity," *Chinese Journal of Geotechnical Engineering*, vol. 22, no. 6, pp. 720–722, 2000.

[36] L. Wang, B. Yao, H. Xie et al., "CO_2 injection-induced fracturing in naturally fractured shale rocks," *Energy*, vol. 139, pp. 1094–1110, 2017.

[37] Y. Xue, S. Liu, J. Chai et al., "Effect of water-cooling shock on fracture initiation and morphology of high-temperature granite: application of hydraulic fracturing to enhanced geothermal systems," *Applied Energy*, vol. 337, no. 337, article 120858, 2023.

[38] L. Wang, Y. Xue, Z. Cao, H. Kong, J. Han, and Z. Zhang, "Experimental study on mode I fracture characteristics of granite after low temperature cooling with liquid nitrogen," *Water*, vol. 15, no. 19, p. 3442, 2023.

[39] Z. Shao, L. Sun, K. R. Aboayanah, Q. Liu, and G. Grasselli, "Investigate the mode I fracture characteristics of granite after heating/-LN2 cooling treatments," *Rock Mechanics and Rock Engineering*, vol. 55, no. 7, pp. 4477–4496, 2022.

[40] T. Yin, Q. Li, and X. Li, "Experimental investigation on mode I fracture characteristics of granite after cyclic heating and cooling treatments," *Engineering Fracture Mechanics*, vol. 222, article 106740, 2019.

[41] L. Yang, J. Z. Li, J. F. Lou et al., "Study on fracture characteristics of coal samples based on notched semi-circular bending tests," *Journal of Mining and Safety Engineering*, vol. 39, no. 5, pp. 1041–1050, 2022.